

Behavior of a test gyroscope moving towards a rotating traversable wormhole

Chandrachur Chakraborty*

Tata Institute of Fundamental Research, Mumbai 400005, India

Parthapratim Pradhan†

Department of Physics, Vivekananda Satabarshiki Mahavidyalaya, West Midnapur 721513 India

Abstract

The geodesic structure of the Teo wormhole is briefly discussed and some observables are derived that promise to be of use in detecting a rotating traversable wormhole indirectly, if it does exist. We also deduce the exact Lense-Thirring (LT) precession frequency of a test gyroscope moving toward a rotating traversable Teo wormhole. The precession frequency diverges on the ergoregion, a behavior intimately related to and governed by the geometry of the ergoregion, analogous to the situation in a Kerr spacetime. Interestingly, it turns out that here the LT precession is inversely proportional to the angular momentum (a) of the wormhole along the pole and around it in the strong gravity regime, a behavior contrasting with its direct variation with a in the case of other compact objects. In fact, divergence of LT precession inside the ergoregion can also be avoided if the gyro moves with a non-zero angular velocity in a certain range. As a result, the spin precession frequency of the gyro can be made finite throughout its whole path, even very close to the throat, during its travel to the wormhole. Furthermore, it is evident from our formulation that this spin precession not only arises due to curvature or rotation of the spacetime but also due to the non-zero angular velocity of the spin when it does not move along a geodesic in the strong gravity regime. If in the future, interstellar travel indeed becomes possible through a wormhole or at least in its vicinity, our results would prove useful in determining the behavior of a test gyroscope which is known to serve as a fundamental navigation device.

1 Introduction

A wormhole or “Einstein-Rosen bridge” is a hypothetical topological feature which would be a shortcut linking two separate points in spacetime. In 1916, Flamm first showed that there can be a tunnel between distant parts of space [1] and such a tunnel is described by the spatial part of the Schwarzschild metric, taken separately from time. Later, Einstein and Rosen also proposed solutions which involve the mathematical representation of the physical space by a space of two identical sheets, a particle being represented by a ‘bridge’ connecting these sheets [2]. So, the wormhole is basically a “tunnel” with two ends and it may connect extremely long distances (say, billions of light years or a part of the Universe with another part sufficiently remote) in a very very short distances (say, within a few meters). The term ‘wormhole’ was first coined by Wheeler in 1957 and he also proposed the concept of the charge-carrying microscopic wormholes [3]. However, the possibility of traversable wormhole was first demonstrated by Ellis [4] in 1973 and independently by Bronnikov [5] in the same year. A duplicate of the Ellis wormholes was presented by Morris and Thorne [6] just as ‘a tool for teaching general relativity’ and they made some important observations. For example, they showed that to stabilize a traversable wormhole, i.e., to hold a wormhole open permanently, one needs exotic matter which must violate the weak energy condition [7]. Later, Visser [8] developed some interesting examples

*chandrachur.chakraborty@tifr.res.in

†pppradhan77@gmail.com

of traversable wormholes to minimize the use of exotic matter and showed that it was possible for a traveler to traverse such a wormhole without passing through a region of exotic matter. Here, we should note that a class of exact stationary and axisymmetric multi-wormhole solutions of the Einstein-Maxwell scalar field equations was generated by Clément [9, 10, 11] and it was shown that these rotating wormhole solutions were asymptotically NUT-like.

Though, wormholes have not been observationally detected till now, Zhou et al. [12] have recently investigated possible observational signatures to identify the astrophysical rotating Ellis wormhole which is basically a massive and compact object. Studying the iron line profile in the X-ray reflected spectrum of a thin accretion disk around the rotating Ellis wormhole, they have found some specific observational signatures which can be used to distinguish the wormhole from the Kerr black hole. Thus, it may be possible to find the wormhole in the near future. In this regard, we calculate some specific observables for Teo wormhole related to the timelike and lightlike geodesics (as the geodesics in Teo wormhole have already been studied in Refs.[13, 14] during the calculation of high energy particle collision and collisional Penrose process in Teo wormhole, we do not want to repeat it here), which may help us to distinguish a rotating traversable wormhole from other compact objects in future, if it in fact exists. Moreover, these observables are also necessary for completeness of our study of the spin precession behavior in Teo wormhole. We will discuss these issues as we proceed.

In this article, we explore how the spin of a gyroscope, a fundamental navigation device, attached to a spaceship, would behave in the vicinity of a wormhole if interstellar travel is possible in future through a traversable wormhole. For our analysis, we consider here the *simplest possible* rotating traversable wormhole which has recently been discovered by Teo [15]. From our analysis the following interesting physical questions could be answered : (i) how will the gyroscope of an astronaut holding his/her spaceship at a constant distance from a wormhole behave? (ii) will the astronaut see any change in behavior of the gyro precession, if the spaceship rotates with some finite angular velocity around the rotating wormhole? (iii)(if the spaceship moves toward an unknown object) can the astronaut distinguish the wormhole from other compact objects, using the behavior of the spin precession of the gyroscope?

To answer the first question, i.e., what an astronaut will see the behavior of the gyro attached to his/her spaceship to be, we have to calculate the Lense-Thirring (LT) precession in Teo wormhole, using the general formulation of LT effect derived in Ref.[16]. We show an ‘adverse effect’ of LT precession in the wormhole spacetime, which can be used to distinguish a rotating traversable wormhole from other compact objects. A more general formulation of the spin precession of a test gyro has recently been derived in Ref.[17], which is more realistic in this sense that the gyro (attached to the spaceship) can move towards the wormhole with an arbitrary angular velocity in a geodesic or non-geodesic path. This will give us answers to the second question as well as partly to the third question.

The paper is organized as follows : in Sec.2, we briefly discuss the timelike and lightlike geodesics in the rotating traversable Teo wormhole and work out the radius of the circular photon orbit (CPO). As an integral part of the study of geodesics, Sec.3 has been devoted to compute the three fundamental frequencies (Kepler frequency, radial and vertical epicyclic frequencies) of a test particle which rotates around the Teo wormhole and using this, we derive the radii of the innermost-stable-circular-orbits (ISCOs). In Sec.4, we derive the exact LT precession frequency of a test gyro which *moves* toward the said wormhole. Using the general formulation of the spin precession [17], we find the behavior of a test gyro (in Sec. 5) which rotates with a non-zero angular velocity around the Teo wormhole or travels toward it. Finally, we conclude in Sec.6.

2 Lorentzian traversable wormhole and Circular Photon Orbit

In this section, we briefly describe the geodesic structure of the traversable wormhole. For this, we first write the metric of the traversable wormhole as [15] :

$$ds^2 = -N^2 dt^2 + \left(1 - \frac{b}{r}\right)^{-1} dr^2 + r^2 K^2 [d\theta^2 + \sin^2 \theta (d\phi - \omega dt)^2] \quad (1)$$

where N, ω, K, b are functions of (r, θ) . This metric is regular on the symmetry axis $\theta = 0, \pi$ and it indicates two identical, asymptotically flat spacetimes which are connected together at the throat, i.e., $r = b > 0$. The discriminant of the metric $D = g_{t\phi}^2 - g_{tt}g_{\phi\phi} = N^2 K^2 r^2 \sin^2 \theta$ indicates that the event horizon can exist for $N = 0$. Since N is finite and also $N \neq 0$ in the case of a wormhole, the event horizon does not exist and the spacetime contains no curvature singularity at all. According to Teo, we can take the parameters N and ω for a particular traversable wormhole as follows [15]:

$$N = K = 1 + \frac{16a^2 d \cos^2 \theta}{r}, \quad \omega = \frac{2a}{r^3} \quad (2)$$

where b and d [13] are positive constants and a is the total angular momentum of the wormhole. The throat of the wormhole occurs at $r = b$ and it looks like a ‘peanut-shell’ (see FIG.1 of Ref.[15]). However, the radial coordinate always satisfies the following condition : $r \geq b$ to maintain the structure of the wormhole spacetime. Therefore, as b determines the spatial shape of the wormhole, b is also called the shape function. For a fast-rotating wormhole $a > \frac{b^2}{2}$ and the ergoregion occurs in the range of $b^2 < r^2 \leq |2a \sin \theta|$. Interestingly, the ergoregion does not extend to the poles (i.e., $\theta = 0$ and $\theta = \pi$), rather it forms a tube like structure around the equatorial plane.

Here, we are mainly interested to derive the radius of CPO in the equatorial plane of the Teo wormhole. Therefore, the metric (Eq. 1) reduces to the following form :

$$ds^2 = - \left(1 - \frac{4a^2}{r^4}\right) dt^2 - \frac{4a}{r} dt d\phi + \left(1 - \frac{b}{r}\right)^{-1} dr^2 + r^2 d\phi^2. \quad (3)$$

To determine the geodesics in the equatorial plane, we follow Refs.[18, 19] and compute the geodesic motion of a neutral test particle setting $\dot{\theta} = 0$ and $\theta = \frac{\pi}{2}$. Therefore, the necessary Lagrangian for the geodesic motion should be

$$2\mathcal{L} = - \left(1 - \frac{4a^2}{r^4}\right) \dot{t}^2 - \frac{4a}{r} \dot{t} \dot{\phi} + \left(1 - \frac{b}{r}\right)^{-1} \dot{r}^2 + r^2 \dot{\phi}^2. \quad (4)$$

The generalized momenta can be written as

$$p_t = - \left(1 - \frac{4a^2}{r^4}\right) \dot{t} - \frac{2a}{r} \dot{\phi} = -\mathcal{E}, \quad (5)$$

$$p_\phi = -\frac{2a}{r} \dot{t} + r^2 \dot{\phi} = \ell, \quad (6)$$

and

$$p_r = \left(1 - \frac{b}{r}\right)^{-1} \dot{r}. \quad (7)$$

Here, \dot{t} , \dot{r} and $\dot{\phi}$ indicate the differentiation with respect to the affine parameter τ . Since the metric does not depend on ‘ t ’ and ‘ ϕ ’, therefore p_t and p_ϕ are conserved quantities. The independence of the metric on ‘ t ’ and ‘ ϕ ’ manifests the stationary and axially symmetric character of the wormhole space-time. However, solving Eq. (5) and Eq. (6) for \dot{t} and $\dot{\phi}$ we obtain

$$\dot{t} = \frac{1}{r^2} \left[\mathcal{E} r^2 - \frac{2a\ell}{r} \right] \quad (8)$$

and

$$\dot{\phi} = \frac{1}{r^2} \left[\frac{2a\mathcal{E}}{r} + \ell \left(1 - \frac{4a^2}{r^4}\right) \right], \quad (9)$$

where \mathcal{E} and ℓ are the energy and angular momentum per unit mass of the test particle, respectively. The normalization condition of the four velocity (u^μ) gives another integral equation for the geodesic motion, which can be written as:

$$g_{\mu\nu}u^\mu u^\nu = \epsilon \quad (10)$$

or

$$-\mathcal{E}\dot{t} + \ell\dot{\phi} + \frac{\dot{r}^2}{(1 - \frac{b}{r})} = \epsilon \quad (11)$$

where $\epsilon = -1$ for time-like geodesics, $\epsilon = 0$ for light-like geodesics and $\epsilon = +1$ for space-like geodesics. Using Eq.(8) and Eq.(9), we eliminate \dot{t} and $\dot{\phi}$ from Eq. (11) and finally we obtain the radial equation that governs the geodesic motion of the test particle in the Teo wormhole as :

$$\dot{r}^2 = \left(1 - \frac{b}{r}\right) \left[\mathcal{E}^2 - \frac{4a\ell\mathcal{E}}{r^3} - \frac{\ell^2}{r^2} + \frac{4a^2\ell^2}{r^6} + \epsilon \right]. \quad (12)$$

For light-like geodesics, we set $\epsilon = 0$ and hence, Eq. (12) reduces to :

$$\dot{r}^2 = \left(1 - \frac{b}{r}\right) \left[\mathcal{E}^2 - \frac{4a\ell\mathcal{E}}{r^3} - \frac{\ell^2}{r^2} + \frac{4a^2\ell^2}{r^6} \right]. \quad (13)$$

We introduce an impact parameter $\eta_c = \frac{\ell_c}{\mathcal{E}_c}$ to determine the radius (r_c) of the unstable CPO for $\mathcal{E} = \mathcal{E}_c$ and $\ell = \ell_c$. Therefore, we obtain two important equations from Eq.(13), which can be written as

$$r_c^6 - \eta_c^2 r_c^4 - 4a\eta_c r_c^3 + 4a^2 \eta_c^2 = 0 \quad (14)$$

and

$$3r_c^3 - 2\eta_c^2 r_c - 6a\eta_c = 0. \quad (15)$$

Now, solving for η_c , we obtain from Eq.(15) :

$$\eta_c = \frac{-3a \pm \sqrt{6r_c^4 + 9a^2}}{2r_c}. \quad (16)$$

Here ‘+’ and ‘-’ signs appear for the direct and retrograde orbits respectively. Now, inserting Eq. (16) in (14), we find the expression to determine the radius of the CPO as,

$$r_c^8 - 15a^2 r_c^4 \pm (ar_c^4 + 12a^3) \sqrt{6r_c^4 + 9a^2} - 36a^4 = 0. \quad (17)$$

Eliminating the square root from the above equation we obtain

$$r_c^{12} - 36a^2 r_c^8 - 1050a^6 = 0 \quad (18)$$

and solving the above equation, the radius of the CPO is determined as

$$r_c \approx \pm 2.4626 \sqrt{a} \quad (19)$$

where the upper sign is applied to the direct orbits and the lower one is applied to the retrograde orbits. Eq.(19) is important for us as it will be applied in Sec.5.2 to calculate the effect of frame-dragging at the CPO.

3 Observables in the rotating traversable wormhole spacetime

It has already been stated that Zhou et al. [12] have recently studied the X-ray reflected spectrum of a thin accretion disk around the rotating Ellis wormhole which is a massive and compact object. They have proposed that the wormholes may look like black holes and they have found some specific observational signatures by which it is possible to distinguish rotating wormholes from Kerr black holes. The Teo traversable wormhole being considered in this article, may not be a compact object but if a test particle moves in this wormhole spacetime it experiences some change in its periodic motion along the co-ordinates r , θ and ϕ . Here, it is necessary to study these periodic variation due to not only the completeness of our study of the geodesic motion of the test particle but also because it helps us to derive the orbital plane precession frequency and the periastron precession frequency which is an integral part of the study of geodesics. If it is possible to detect the wormhole in near future and if we want to conduct realistic experiments in the rotating wormhole spacetime then these precession frequencies will serve as observables. The periodic motion along r and θ of a test particle is known as radial epicyclic frequency and vertical epicyclic frequency respectively. The periodic variation along ϕ is very well-known to us, it is the Kepler frequency.

At first, we consider a general stationary and axisymmetric spacetime as follows:

$$ds^2 = g_{tt}dt^2 + 2g_{t\phi}d\phi dt + g_{\phi\phi}d\phi^2 + g_{rr}dr^2 + g_{\theta\theta}d\theta^2 \quad (20)$$

where $g_{\mu\nu} = g_{\mu\nu}(r, \theta)$. In this spacetime, the proper angular momentum (l) of a test particle can be defined as :

$$l = -\frac{g_{t\phi} + \Omega_\phi g_{\phi\phi}}{g_{tt} + \Omega_\phi g_{t\phi}} \quad (21)$$

where, Ω_ϕ is the Kepler frequency of the test particle which is defined as [20]

$$\Omega_\phi = \frac{d\phi/d\tau}{dt/d\tau} = \frac{d\phi}{dt} = \frac{-g'_{t\phi} \pm \sqrt{g'^2_{t\phi} - g'_{tt}g'_{\phi\phi}}}{g'_{\phi\phi}} \Big|_{r=\text{constant}, \theta=\text{constant}} \quad (22)$$

where the prime denotes the partial differentiation with respect to r .

For Teo rotating traversable wormhole (Eq.(3)) we can calculate the Kepler frequency which comes out as,

$$\Omega_\phi^d = \frac{2a}{r^3} \quad (23)$$

and

$$\Omega_\phi^g = -\frac{4a}{r^3}. \quad (24)$$

where the negative sign indicates that the rotation is in the reverse direction. Suffixes d and g stand for the direct and retrograde rotation respectively.

The general expressions for calculating the radial (Ω_r) and vertical (Ω_θ) epicyclic frequencies are [20]

$$\begin{aligned} \Omega_r^2 &= \frac{(g_{tt} + \Omega_\phi g_{t\phi})^2}{2 g_{rr}} \partial_r^2 U \\ &= \frac{(g_{tt} + \Omega_\phi g_{t\phi})^2}{2 g_{rr}} [\partial_r^2 (g_{\phi\phi}/Y) + 2l \partial_r^2 (g_{t\phi}/Y) + l^2 \partial_r^2 (g_{tt}/Y)] \Big|_{r=\text{const.}, \theta=\text{const.}} \end{aligned} \quad (25)$$

and

$$\begin{aligned}\Omega_\theta^2 &= \frac{(g_{tt} + \Omega_\phi g_{t\phi})^2}{2 g_{\theta\theta}} \partial_\theta^2 U \\ &= \frac{(g_{tt} + \Omega_\phi g_{t\phi})^2}{2 g_{\theta\theta}} [\partial_\theta^2 (g_{\phi\phi}/Y) + 2l \partial_\theta^2 (g_{t\phi}/Y) + l^2 \partial_\theta^2 (g_{tt}/Y)]|_{r=const., \theta=const.}\end{aligned}\quad (26)$$

respectively and Y can be defined as

$$Y = g_{tt}g_{\phi\phi} - g_{t\phi}^2. \quad (27)$$

In our case, we are confined to $\theta = \pi/2$ which is physically reliable. Thus, we obtain for the Teo wormhole

$$Y = -r^2 \quad (28)$$

for $\theta = \pi/2$ and

$$\partial_r^2 U|_{r=r_{const}, \theta=\pi/2} = \frac{6l}{r^8} (lr^4 - 28a^2l + 8ar^3). \quad (29)$$

As the proper angular momentum are calculated for this particular wormhole as

$$l^d = 0 \quad (30)$$

and

$$l^g = \frac{6ar^3}{12a^2 - r^4} \quad (31)$$

we obtain the radial epicyclic frequencies (Ω_r) from Eq.(25) for the direct and retrograde rotation as

$$\Omega_r^{2(d)} = 0 \quad (32)$$

and

$$\Omega_r^{2(g)} = -\frac{36a^2(1 - \frac{b}{r})}{r^{10}} (r^4 + 36a^2) \quad (33)$$

respectively.

3.1 Radius of the innermost stable circular orbits (ISCOs)

It is well-known that the square of the radial epicyclic frequency is equal to zero at the ISCO and it is negative for the smaller radius, which shows the radial instabilities for orbits with radius smaller than the ISCO. In our case, it is easily seen from Eq.(33) that $\Omega_r^{2(g)}$ vanishes at $r = b$ ($r = b$ is actually the radius of the throat of the wormhole) but it becomes negative for $r > b$. This means that only one stable circular orbit is possible at $r = b$ for the retrograde rotation and the orbits occurred at $r > b$ are unstable. Thus, ISCO is meaningless in this particular case. On the other hand, Eq.(32) reveals that the radial epicyclic frequency vanishes for all direct orbits. This means that all direct orbits are stable in the Teo wormhole spacetime and no instability is there. Thus, ISCO should occur at $r = b$ for the timelike geodesics and it could be stated that the ISCO coincides at the throat of the Teo wormhole in case of the prograde rotation. Here, we can note that the ISCO coincides at the throat [12] for the direct orbit in case of a rotating Ellis wormhole also.

3.2 Periastron precession frequency

It is very surprising that the radial epicyclic frequency vanishes for the direct orbit as the angular momentum is zero in this case. Interestingly, the angular velocity is non zero (Eq.(23)) for the direct orbit, which can be an example of the zero angular momentum observer with non-zero angular velocity. Therefore, if a test particle rotates in any circular geodesic (direct orbit) in this spacetime, it will carry zero angular momentum with non-zero angular velocity. Now, we can easily calculate the *periastron precession rate* (Ω_{per}^d) for the direct orbit which turns out to be

$$\Omega_{\text{per}}^d = \Omega_{\phi}^d - \Omega_r^d = \Omega_{\phi}^d = \frac{2a}{r^3}. \quad (34)$$

Thus, it is really remarkable that the periastron precession rate is equal to the Kepler frequency (Eq.23) for the direct orbit in the Teo wormhole. This means that the precession rate of the orbit (Ω_{per}^d) of the test particle is same as the angular velocity of it. But, for the retrograde rotation the *periastron precession frequency* comes out as

$$\Omega_{\text{per}}^g = \Omega_{\phi}^g - \sqrt{|\Omega_r^2{}^{(g)}|} = -\frac{2a}{r^3} \left[2 + \frac{3}{r^2} \left(1 - \frac{b}{r} \right)^{\frac{1}{2}} (r^4 + 36a^2)^{\frac{1}{2}} \right]. \quad (35)$$

Negative sign confirms that the rotation is in the reverse direction.

3.3 Orbital plane precession frequency

To calculate the orbital plane precession frequency, we first have to obtain the vertical epicyclic frequency for the Teo wormhole and for that we calculate

$$\partial_{\theta}^2 U|_{r=r_{\text{const}}, \theta=\pi/2} = \frac{64a^2d}{r} - l \frac{128a^3d}{r^4} + \frac{2l^2}{r^2} \left[1 - \frac{32a^2d}{r} \left(1 - \frac{4a^2}{r^4} \right) \right]. \quad (36)$$

Now, substituting it into Eq.(26) and also taking the values of l from Eq.(30,31) we obtain

$$\Omega_{\theta}^2{}^{(d)} = \frac{32a^2d}{r^3} \quad (37)$$

for the direct orbit and for the retrograde orbit we obtain

$$\Omega_{\theta}^2{}^{(g)} = \frac{4a^2}{r^7} [9r + 8d(r^4 - 36a^2)]. \quad (38)$$

As it has already been derived the exact Kepler frequencies and the vertical epicyclic frequencies of a test particle which rotates in a circular orbit around the traversable wormhole in the equatorial plane, now we can obtain the *nodal precession frequency* (Ω_{nod}) easily. It is also called as the orbital plane precession frequency or the Lense-Thirring (LT) precession frequency of a *test particle*. Using Eqs.(23,24) and Eqs.(37,38) we obtain :

$$\Omega_{\text{nod}}^d = \Omega_{\phi}^d - \Omega_{\theta}^d = \frac{2a}{r^3} (1 - \sqrt{8r^3d}) \quad (39)$$

for the direct orbit and for the retrograde orbit it comes out as

$$\Omega_{\text{nod}}^g = \Omega_{\phi}^g - \Omega_{\theta}^g = -\frac{2a}{r^3} \left[2 + \left(9 + \frac{8d}{r} (r^4 - 36a^2) \right)^{\frac{1}{2}} \right] \quad (40)$$

where the negative sign indicates that the rotation is in the reverse direction.

It is important to mention here that Eq.(34) and Eq.(39) are physically meaningful as the stable circular orbits exist for $r \geq b$ but Eq.(35) and Eq.(40) are not important except that particular orbit occurred at $r = b$ because only this orbit is stable.

4 Lense-Thirring precession of a test gyro in the rotating traversable wormhole spacetime

We are keen to derive the Lense-Thirring (LT) precession [21] frequency of a test gyro [22] in a general rotating traversable wormhole spacetime, which could be regarded as a more realistic observable for the indirect detection of a wormhole. In 2004, NASA sent the Gravity Probe B (GP-B) satellite to measure the Geodetic and LT precession frequencies of a test gyro due to the rotation of the earth and the result had been published by Everitt et al. in 2011 [23]. It may play an important role in the future astrophysical observational purpose to measure the LT precession frequency of a wormhole to distinguish its nature from the other compact objects as well. We note that the exact LT precession rate of a test gyro in the Kerr spacetime [16] and some other axisymmetric spacetimes [24, 25] have already been derived. Now, this formulation can also be applied to obtain the frame-dragging effect in case of the rotating wormhole as well. The canonical metric for a general stationary, axisymmetric traversable wormhole has been written in Eq.(1). Using this metric, the exact LT precession rate of a test gyro relative to the Copernican system (or ‘fixed stars’) in the rotating traversable wormhole spacetime can be expressed in the orthonormal coordinate basis as:

$$\begin{aligned} \vec{\Omega}_{LT} = & \frac{1}{2NK(-N^2 + \omega^2 r^2 K^2 \sin^2 \theta)} \cdot \\ & \left[K \left(1 - \frac{b}{r} \right)^{1/2} \sin \theta [N^2 (Kr\omega_{,r} + 2\omega r K_{,r} + 2\omega K) + \omega^2 r^3 K^3 \omega_{,r} \sin^2 \theta - 2\omega Kr N N_{,r}] \hat{\theta} \right. \\ & \left. - [N^2 (K\omega_{,\theta} \sin \theta + 2\omega K_{,\theta} \sin \theta + 2\omega K \cos \theta) + \omega^2 r^2 K^3 \omega_{,\theta} \sin^3 \theta - 2\omega K N N_{,\theta} \sin \theta] \hat{r} \right] \end{aligned} \quad (41)$$

and the modulus of the above LT precession rate is

$$\begin{aligned} \Omega_{LT} = & |\vec{\Omega}_{LT}(r, \theta)| \\ = & \frac{1}{2NK(-N^2 + \omega^2 r^2 K^2 \sin^2 \theta)} \cdot \\ & \left[K^2 \left(1 - \frac{b}{r} \right) \sin^2 \theta [N^2 (Kr\omega_{,r} + 2\omega r K_{,r} + 2\omega K) + \omega^2 r^3 K^3 \omega_{,r} \sin^2 \theta - 2\omega Kr N N_{,r}]^2 \right. \\ & \left. + [N^2 (K\omega_{,\theta} \sin \theta + 2\omega K_{,\theta} \sin \theta + 2\omega K \cos \theta) + \omega^2 r^2 K^3 \omega_{,\theta} \sin^3 \theta - 2\omega K N N_{,\theta} \sin \theta]^2 \right]^{\frac{1}{2}}. \end{aligned} \quad (42)$$

4.1 LT precession of a test gyro in the Teo wormhole

According to Teo, we can take N and ω as the following:

$$N = K = 1 + \frac{16a^2 d \cos^2 \theta}{r}, \quad \omega = \frac{2a}{r^3} \quad (43)$$

and can calculate the exact LT precession rate of a test gyro for the said wormhole, which can be expressed as

$$\vec{\Omega}_{LT} = \frac{a}{Nr^3 \left(1 - \frac{4a^2}{r^4} \sin^2 \theta \right)} \cdot \left[N \sin \theta \left(1 - \frac{b}{r} \right)^{\frac{1}{2}} \left(1 + \frac{12a^2}{r^4} \sin^2 \theta \right) \hat{\theta} + 2 \cos \theta \hat{r} \right]. \quad (44)$$

Along the pole we can take $\theta = 0$ and the LT precession frequency can be obtained as

$$|\vec{\Omega}_{LT}| = \frac{2a}{r^2(r + 16a^2 d)}. \quad (45)$$

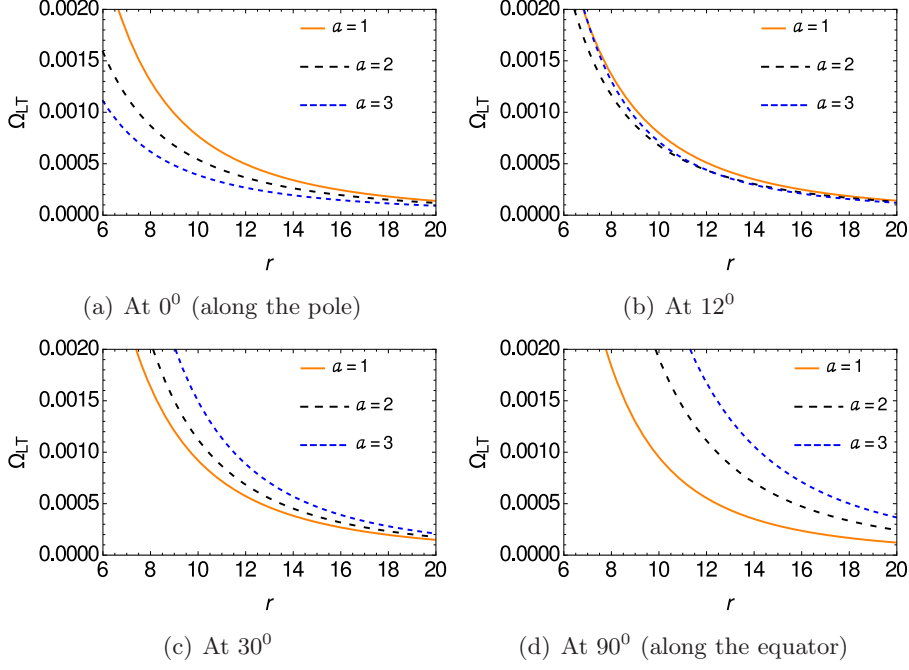


Figure 1: Radial variation of the LT precession frequency ($\Omega_{LT} = |\vec{\Omega}_{LT}|$) in the Teo wormhole for $b = 1$ & $d = 1$

Similarly, we can take $\theta = \pi/2$ along the equator and the LT precession frequency comes out as

$$|\vec{\Omega}_{LT}| = \frac{a}{r^3 \left(1 - \frac{4a^2}{r^4}\right)} \cdot \left(1 - \frac{b}{r}\right)^{\frac{1}{2}} \left(1 + \frac{12a^2}{r^4}\right) \hat{\theta}. \quad (46)$$

Weak field approximation ($r \gg \sqrt{a}$) can be taken at a large distance, for which Eq.(44) reduces to

$$\vec{\Omega}_{LT} = \frac{a}{Nr^3} \cdot \left[N \sin \theta \left(1 - \frac{b}{r}\right)^{\frac{1}{2}} \hat{\theta} + 2 \cos \theta \hat{r} \right]. \quad (47)$$

Here, we should note that the LT precession formulation is valid only outside the ergoregion [16] as an observer cannot remain stationary with zero angular velocity. Thus, Eq.(44) and the related equations will valid only in the following range:

$$r \geq b \quad \text{and} \quad r^2 > 2a \sin \theta \quad (48)$$

and both of the above conditions must be hold. As we have stated earlier that the ergoregion (r_e) occurs for the rotating Teo wormhole in this range $b < r_e \leq \sqrt{2a \sin \theta}$, the calculation of LT precession frequency is valid only for $r > \sqrt{2a \sin \theta}$. It should be noticed that the ergoregion does not fully surround the throat but forms a tube around the equatorial region of the said wormhole. Unlike a rotating black hole spacetime, the ergoregion of a rotating wormhole does not coincide with the horizon at the pole as the event horizon does not exist in this spacetime at all. At the equatorial plane, the ergoregion is extended upto $r_e = \sqrt{2a}$ and it decreases slowly if we move to the pole from the equator. Finally, the ergoregion vanishes ($r_e = 0$) at the pole for $\theta = 0$.

In Fig.1, we have plotted the LT precession frequencies (44) of the Teo wormhole to see the graphical nature of it. It can be seen from panel (a) of Fig.1 that the LT precession frequency (Ω_{LT}) decreases along the pole with increasing the angular momentum (a) of the spacetime. This is remarkable in this sense that the LT precession frequency varies inversely with the rotation of the spacetime or so-called

the angular momentum of the spacetime. Generally, frame-dragging rate varies directly with a in case of the black holes and pulsars but in case of a rotating traversable wormhole its behaviour is slightly different. The evolution of the frame-dragging rate has been shown in panel (a)-(d) of Fig.1. If we move from the pole to the equator, the blue line comes upward in a faster rate than the orange one and the three colors are slightly indistinguishable in panel (b) which is drawn for $\theta = 12^\circ$. After crossing the angle $\theta \sim 15^\circ$ with respect to the pole, the three colors are distinguishable and we can see that the orange line comes down and blue line comes up which is the general trend as it was generally known to us that if we increase the rotation of the spacetime frame-dragging rate increases. In this sense, the nature of the plots of Panels (c) and (d) is expected but the nature of the plots of Panels (a) and (b) is quite unexpected. Frame-dragging behaves differently only along the pole and its nearby region ($\sim 10^\circ$) at the strong gravity regime in the wormhole spacetime. In case of the weak field limit ($r \gg \sqrt{a}$), it does not behave differently along the pole, we mean, the frame-dragging rate decreases with decreasing the rotation of the spacetime not only along the pole but also along the equator of this wormhole spacetime like the other compact objects ($\Omega_{LT} \propto a/r^3$) which is evident from Eq.(45) and Eq.(46). In the weak-field limit Eq.(45) and Eq.(46) reduce to

$$|\Omega_{LT}|_{\theta=0}^{\text{weak}} \approx \frac{2a}{r^3} \quad (49)$$

and

$$|\Omega_{LT}|_{\theta=\pi/2}^{\text{weak}} \approx \frac{a}{r^3} \quad (50)$$

respectively, which is expected. Even in the weak gravity regime of the Kerr spacetime, LT precession rates of a test gyro reduce to $2a/r^3$ along the pole and a/r^3 along the equator. That is why, $\Omega_{LT} \propto a$ and $\Omega_{LT} \propto r^{-3}$ in case of all compact objects as well as in case of the wormholes. Therefore, the weak-field limit of LT precession cannot distinguish a wormhole from the other compact objects but strong field LT precession can do that. Because, in the strong gravity regime of a rotating wormhole ($r \lesssim \sqrt{a}$), Eq.(45) and Eq.(46) reduce to¹

$$|\Omega_{LT}|_{\theta=0}^{\text{strong}} \approx \frac{1}{8ar^2} \quad (51)$$

and

$$|\Omega_{LT}|_{\theta=\pi/2}^{\text{strong}} \approx \frac{3a}{r^3} \left(1 - \frac{b}{r}\right)^{\frac{1}{2}} \quad (52)$$

respectively. It is evident from Eq.(51) that Ω_{LT} along the pole is proportional to a^{-1} instead of a and this adverse effect nullifies at the distance $r \sim 16a^2$ (can be obtained using Eq.(49) and Eq.(51)) along the pole. It is also interesting to notice that Ω_{LT} is proportional to r^{-2} instead of r^{-3} along the pole. This anomaly exists only along the pole of the wormhole and this anomaly vanishes very quickly as we move from the pole to the equator. We can see from Eq.(52) that no special anomaly arises in the expression of Ω_{LT} along the equator where Ω_{LT} varies as a/r^3 . It is also seen from the plots (Fig.1) that the value of the LT precession rate along the pole is quite lower than its value along the equator. Thus, if an astronaut wants to travel through the wormhole, he/she does not see the higher precession rate of the gyroscope attached to his/her spaceship (relative to the precession rate along the equator) due to the frame-dragging effect, even if the wormhole rotates very fast as the rapidly rotating wormhole drags its nearby spacetime ($r \sim 16a^2$) slowly.

This same anomaly should not be appeared in case of the Kerr black hole or other axisymmetric spacetimes like other black holes and pulsars. In the Kerr spacetime, the boundary of the outer ergoregion occurs at $r_e = M + \sqrt{M^2 - a^2/M^2 \cos^2 \theta}$ where a can take value from 0 to M^2 ($0 < a \leq M^2$). Thus, if we take the limit $r < \sqrt{a}$ (Eq.(42) of [16]), it will be inside the ergoregion, which is

¹we have taken $d = 1$ following Refs.[15, 13]

unphysical and also beyond the frame-dragging formulation as it is valid only in the timelike region, we mean, outside the ergoregion. Thus, we cannot consider the region $r < \sqrt{a}$ which is basically invalid and the region is inside the ergosphere. In case of the wormhole, there is no horizon and the LT formulation is valid for the range $r > \sqrt{2a \sin \theta}$. Now for $\theta = 0$, the LT formulation is valid in $r \geq b$ along the pole and for $r > \sqrt{2a}$ along the equator and so on. Thus, it is meaningful to calculate the LT precession rate for any real distance equal to the throat radius or greater than this ($r \geq b$) along the pole of the wormhole spacetime. In this situation, if we calculate the LT precession rate in the region $b \leq r \sim 16a^2$ using Eq.(44), we can see that the LT precession rate decreases with increasing the rotation of the wormhole spacetime but this treatment is not applicable for all the angles as r must be greater than $\sqrt{2a \sin \theta}$.

It could be noted here that we found an ‘anomaly’ in LT precession in Kerr-Taub-NUT spacetime [26] and inside the pulsars [25, 27] where LT precession does not always follow the inverse cube law of distance but the LT precession was proportional to the rotation of those spacetime everywhere. This is first time when we have found a completely different ‘anomaly’ in the LT precession, which is related to the intrinsic rotation of the spacetime.

5 Spin precession of the test gyro in Teo wormhole : general formalism

In the previous section, we have shown that the spin precession of a test gyro, which arises due to the LT effect and diverges on the ergoregion. This behavior is similar to the cases of Kerr black hole and Kerr naked singularity [16, 28]. Interestingly, it has recently been shown in [28] that this behavior is intimately related to and is governed by the geometry of the ergoregion in case of a Kerr spacetime. In this regard, we should discuss the structure of the ergoregion of a Teo wormhole as well. After that, we will proceed to derive the general formalism of the spin precession in Teo wormhole so that it can be applied inside as well as outside of the ergoregion.

5.1 Ergoregion in Teo Wormhole and its comparison with Kerr spacetime

Teo pointed out that the ergoregion occurs in the range : $b < r_e \leq \sqrt{2a \sin \theta}$ in case of the said wormhole. According to him, ergoregion could not extend to the poles but it forms a tube like structure around the equatorial plane. We find that the structure of the ergoregion extends actually in the following angular range : $\sin^{-1} \frac{b^2}{2a} \leq \theta_e \leq \pi/2$ and $-\sin^{-1} \frac{b^2}{2a} \geq \theta_e \geq -\pi/2$ whereas ergoregion absent in the following range :

$$-\sin^{-1} \frac{b^2}{2a} < \theta_{ne} < \sin^{-1} \frac{b^2}{2a} \quad (53)$$

where θ_e is the angular range which is inside the ergoregion and $2\theta_{ne} (\equiv 2 \sin^{-1} \frac{b^2}{2a})$ is the ‘opening angle’, i.e., ergoregion is absent in this portion. Therefore, a gyro gets an accessible angular cone around the polar axis to enter inside the wormhole without touching the ergoregion. This is necessary for a static observer (whose angular velocity is zero), which has been considered in Sec.4.1 to derive the LT precession. For an example, if $a = b = 1$, the ergoregion extends in the following ranges : $\pi/6 \leq \theta_e \leq \pi/2$ and $-\pi/6 \geq \theta_e \geq -\pi/2$ whereas ergoregion absent for $-\pi/6 < \theta_{ne} < \pi/6$. Therefore, the ‘opening angle’ is $\pi/3$ in this example. However, Eq.(53) reveals that the volume of the ergoregion increases with increasing the angular momentum (a) of the wormhole, i.e., the volume of the “tube” around the equatorial region increases. For $a \rightarrow \infty$, ergoregion extends upto $-\pi/2 \leq \theta_e \leq \pi/2$ in principle, which means that the opening angle (θ_{ne}) completely vanishes in this case. This is in stark contrast with Kerr naked singularity case where it has been shown that the volume of the ergoregion decreases with increasing the angular momentum of the Kerr spacetime (see Eq.(4) of [28]) and the volume becomes zero for infinite angular momentum, in principle. Interestingly, the “tube” like structure of the ergoregion around the equatorial plane is also formed in case of a Kerr naked singularity (see FIG. 1 and FIG. 2 of [28]), which is quite similar to the rotating Teo wormhole case.

Only one difference is that, the radius of the region enclosed by the “tube” (throat) is $r = b$ (this value does not depend on the value of angular momentum a) at the equatorial plane in case of Teo wormhole whereas this is equal to the Kerr parameter (radius of the ring singularity) in case of Kerr naked singularity (see FIG. 2 of [28]).

5.2 Derivation of the spin precession frequency

In Sec.4.1, we have shown that the LT precession does not follow the ‘usual behavior’ in the strong gravity regime of a rotating wormhole. It could also be noted that the strong gravity LT formulation does not valid inside the ergoregion as an observer cannot remain stationary there with zero angular velocity. To remain fixed at a particular r and θ inside the ergoregion, the astronaut has to rotate with an angular velocity Ω within a certain range, so that the velocity of the observer is timelike. Using this idea, the more general formulation of the spin precession of a test gyro is recently developed in Ref. [17]. This formulation is valid not only inside the ergoregion but also outside of it. If a test gyro moves with Ω , the spin precession frequency of it can be calculated using this formulation but we should remember that this precession does not arise due to only the LT effect. Some additional precessions are also included with it. We will discuss it as we proceed. Here, we recapitulate the general formulation of the spin precession which is valid in any stationary and axisymmetric spacetime and can be expressed as (Eq.14 of [17])

$$\begin{aligned} \vec{\Omega}_p = & \frac{1}{2\sqrt{-g} \left(1 + 2\Omega \frac{g_{0\phi}}{g_{00}} + \Omega^2 \frac{g_{\phi\phi}}{g_{00}} \right)} \cdot \\ & \left[-\sqrt{g_{rr}} \left[\left(g_{0\phi,\theta} - \frac{g_{0\phi}}{g_{00}} g_{00,\theta} \right) + \Omega \left(g_{\phi\phi,\theta} - \frac{g_{\phi\phi}}{g_{00}} g_{00,\theta} \right) + \Omega^2 \left(\frac{g_{0\phi}}{g_{00}} g_{\phi\phi,\theta} - \frac{g_{\phi\phi}}{g_{00}} g_{0\phi,\theta} \right) \right] \hat{r} \right. \\ & \left. + \sqrt{g_{\theta\theta}} \left[\left(g_{0\phi,r} - \frac{g_{0\phi}}{g_{00}} g_{00,r} \right) + \Omega \left(g_{\phi\phi,r} - \frac{g_{\phi\phi}}{g_{00}} g_{00,r} \right) + \Omega^2 \left(\frac{g_{0\phi}}{g_{00}} g_{\phi\phi,r} - \frac{g_{\phi\phi}}{g_{00}} g_{0\phi,r} \right) \right] \hat{\theta} \right]. \end{aligned} \quad (54)$$

It could be noticed from Eq.(54) that $\vec{\Omega}_p$ reduces to the LT precession equation ($\vec{\Omega}_p|_{\Omega=0} = \vec{\Omega}_{LT}$) if Ω vanishes. Otherwise, using Eq.(54) we can obtain LT precession frequency plus some additional frequencies which arise due to the non-zero angular velocity of the gyro. For an example, LT precession frequency is zero in the Schwarzschild spacetime as it is non-rotating but the geodetic precession does not vanish in the Schwarzschild spacetime, which arises due to the non-zero curvature of the spacetime or we can say that it is an effect of the non-zero mass ($M \neq 0$) of the spacetime. If a gyro rotates in a circular geodesic around a Schwarzschild spacetime, Ω should be the Kepler frequency : $\Omega = (M/r^3)^{\frac{1}{2}}$. Thus, the geodetic precession arises due to the non-zero M or in a broader sense, due to the non-zero angular velocity Ω . Setting $g_{0\phi} = 0$ and $\Omega = \text{Kepler frequency}$ in Eq.(54), one can obtain the geodetic precession frequency in a non-rotating spacetime. This has already been explained in Section IV-C of Ref.[17] in detail. In Kerr spacetime, the total precession frequency is obtained using the full expression of Eq.(54) as the LT precession and geodetic precession both are non-vanishing in this case. However, we can apply Eq.(54) to obtain the total spin precession frequency in Teo wormhole but we have to choose a suitable range of Ω for it. Basically, outside as well as inside of the ergoregion, Ω can take any value, provided that the four-velocity ($u = u_{\text{obs}}^\alpha = u_{\text{obs}}^t (1, 0, 0, \Omega)$) of the gyro be timelike. Therefore, the range of Ω is calculated as [17]:

$$\Omega_-(r, \theta) < \Omega < \Omega_+(r, \theta) \quad (55)$$

where,

$$\Omega_\pm = \omega \pm \frac{1}{r \sin \theta} = \frac{2a}{r^3} \pm \frac{1}{r \sin \theta} \quad (56)$$

in case of the Teo wormhole. Otherwise, the gyro cannot remain stationary inside of the ergoregion. For simplicity, we introduce a parameter q to scan the allowed values for Ω inside the ergoregion

($b < r \leq \sqrt{2a \sin \theta}$) of the said wormhole, which follows

$$\Omega = q \Omega_+ + (1 - q) \Omega_- = \Omega = \omega + \frac{(2q - 1)}{r \sin \theta} \quad (57)$$

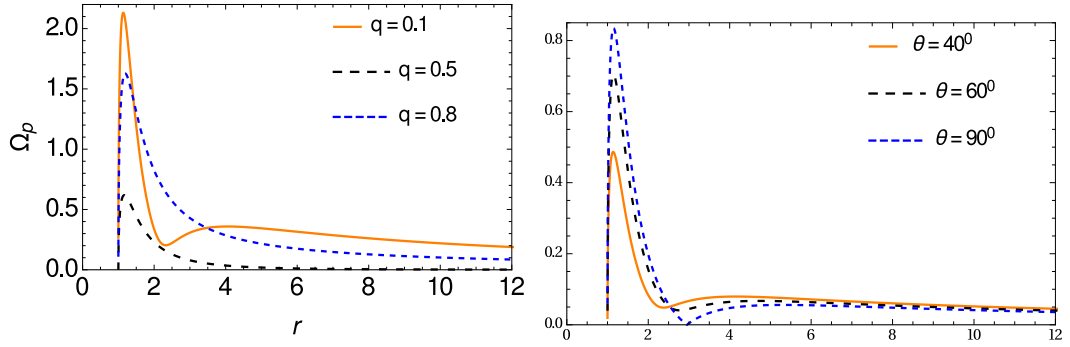
where $0 < q < 1$. Now, in case of a Teo wormhole, we can express the total spin precession frequency of a test gyro (which rotates with an arbitrary Ω) as

$$\begin{aligned} \vec{\Omega}_p = & \frac{1}{4q(1 - q) N r^3} \cdot [(2a - \Omega r^3) \cos \theta \hat{r} \\ & + N \sin \theta \left(1 - \frac{b}{r}\right)^{\frac{1}{2}} \left\{ a \left(1 + \frac{12a^2}{r^4} \sin^2 \theta\right) + \Omega r^3 \left(1 - \frac{12a^2}{r^4} \sin^2 \theta\right) + 3ar^2 \Omega^2 \sin^2 \theta \right\} \hat{\theta}]. \end{aligned} \quad (58)$$

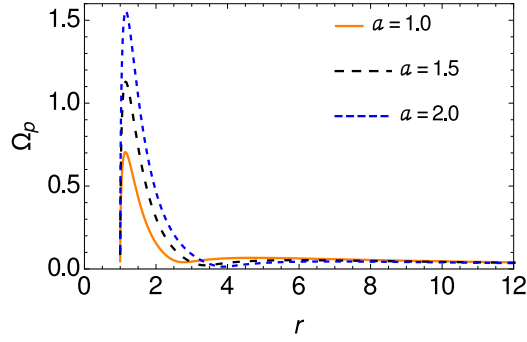
We note that the above expression is valid for $r \geq b$ and $0 < \theta \leq \pi/2$. Teo wormhole is a *simplest* possible rotating traversable wormhole in this sense that only the throat radius b and angular momentum a have been introduced in it. Therefore, it is possible to identify the effect of these two parameters in the spin precession, which is quite interesting. Teo wormhole is not explicitly depend on the mass parameter of the spacetime, which is basically responsible for the geodetic precession in Schwarzschild and Kerr spacetimes. Eq.(58) reveals that the spin precession arises due to the frame-dragging effect as well as the non-zero rotation (Ω) of the spin. As a special case, if the gyro rotates in a circular geodesic in the Schwarzschild spacetime, Ω arises due to the non-zero mass. Thus, Ω_p gives the geodetic precession frequency. Now, if the gyro rotates in a circular geodesic of a *non-rotating* ($a = 0$) Teo wormhole, it can easily be shown using Eq.(23) and Eq.(24) that Ω_p vanishes as Kepler frequency ($\propto a/r^3$) depends solely on the angular momentum (a) of the wormhole. We argue that as the Teo wormhole or the Kepler frequency has no explicit mass dependence, geodetic precession does not arise in this case. It is needless to say here that LT precession is zero as the spacetime is non-rotating. Therefore, an astronaut does not see any precession of the test spin/gyro attached to his/her spaceship in this case. This interesting phenomena is completely absent in the cases of other compact objects. If the gyro does not move along a geodesic (as it pointed out earlier in Refs. [29, 30] that a gyro does not move along the geodesic in strong gravity), Ω may not be zero even in case of $a = 0$. It can be seen from Eq.(57) that the angular velocity of the stationary observer Ω reduces to $\Omega = (2q - 1)/(r \sin \theta)$ when it moves toward a non-rotating wormhole ($a = 0$) spacetime. Therefore, the spin precession arises due to only the rotation of the test gyro in this case. We are not interested in the non-rotating wormhole in our present article but what we want to emphasize it here is that the spin precession not only arises due to the curvature of the spacetime or rotation of the spacetime but it also arises due to the non-zero angular velocity of the spin when it does not move along a geodesic in the strong gravity regime. This special effect is absent if the gyro moves along a geodesic.

In Fig.2 we plot the radial variation of the spin precession frequency $\Omega_p = |\vec{\Omega}_p|$ to see the nature of the spin precession in Teo wormhole. The ergoregion extends from $b < r_e \leq \sqrt{2a \sin \theta}$ in all the plots where we have taken $b = 1$ and the maximum and minimum values of a are taken as $a = 2$ and $a = 1$ respectively. Thus, the ergoregion occurs in the following ranges : $1 < r_e \leq 1.86$ for $a = 2$ and $1 < r_e \leq 1.31$ for $a = 1$ at $\theta = 60^\circ$. Panel (a) shows the radial variation of Ω_p for three different values of q . It is clearly seen from this plot that a local maxima and a local minima appear for $q = 0.1$. Actually, this anomaly occurs for any value of q : $0 < q < 0.5$ but it is absent for $0.5 \leq q < 1$. If q increases from 0 to 0.5, the value of Ω_p decreases and the local maxima (r_x) and minima (r_n) disappear for $q = 0.5$. Further increment of q from 0.5 to 1, the value of Ω_p increases but the local maxima and minima do not appear again. Panel (b) shows that the spin precession rate increases at $r = r_x$ and it decreases for $r \geq r_n$, if the gyro moves from the pole to the equator of the wormhole. Panel (c) shows that Ω_p is higher for higher a at the local maxima but it is completely opposite for $r = r_n$. The later feature is quite similar to Panel (a) and Panel (b) of Fig.1. We note that the spin precession frequency at the throat of rotating Teo wormhole is

$$\vec{\Omega}_p|_{r \rightarrow b} \rightarrow \frac{(1 - 2q) \cot \theta \hat{b}}{4q(1 - q) (b + 16a^2 d \cos^2 \theta)} \quad (59)$$



(a) For three different values of q at $\theta = 60^\circ$ with $a = 1$ (b) In three different angles with $a = 1$ and $q = 0.3$



(c) For three different values of a at $\theta = 60^\circ$ with $q = 0.3$

Figure 2: Plot of spin precession frequency (Ω_p) of a test gyro vs distance (r) for three different circumstances in the wormhole spacetimes for $b = 1$ & $d = 1$

which vanishes for $q = 0.5$ (see Panel (a) of Fig.2) or $\theta = \pi/2$. It could be noticed from Eq.(59) that the spin precession does not vanish even if $a = 0$ but it vanishes for $q = 0.5$ as in that case Ω_p arises due to frame-dragging effect only. We discuss it vividly in the next section.

5.3 Special Case : ZAMO

$q = 0.5$ is a very special case which is also quite interesting in general relativity as well as in Astrophysics. For $q = 0.5$, Eq.(57) reduces to

$$\Omega = \omega = \frac{2a}{r^3}. \quad (60)$$

Only in this case, the test gyro can regard the $+\phi$ and $-\phi$ directions as equivalent in terms of the local geometry. This can also be said as the gyro is “non-rotating relative to the local spacetime geometry” or we can say it as “locally non-rotating observer/gyro” who moves with the angular velocity $\Omega = \omega$. Thus, the angular momentum of this “locally non-rotating observer” is zero, for which the observer is called as the Zero-Angular-Momentum-Observer (ZAMO) which was first introduced by Bardeen [31, 32]. Bardeen et al.[33] showed that the ZAMO could be a powerful tool in the analysis of physical processes near astrophysical object. It is needless to say that our general expression (Eq.54) of spin precession is valid not only for $q = 0.5$ but also for all possible values of the angular momentum (Ω) of the gyro, i.e., $0 < q < 1$. However, as it has been described in Refs.[34, 32] that the angular velocity of the photon could be expressed by ω , one can calculate in principle the spin precession frequency using our general expression Eq.(58). This can be written as :

$$\vec{\Omega}_p|_{q=1/2} = \frac{3a \sin \theta \left(1 - \frac{b}{r}\right)^{\frac{1}{2}}}{r^3} \hat{\theta}. \quad (61)$$

The above expression (Eq.61) reveals that the spin precession frequency is directly proportional to a , which means that the spin precession arises in this case due to only the frame-dragging effect, i.e., the non-zero rotation of the spacetime. In some articles, ZAMO has been introduced to derive the frame-dragging effect in this special situation (for an example, see Ref.[35] where the frame-dragging frequency was derived for rapidly rotating neutron stars using ZAMO). Earlier, we derived the radius of CPO at the equatorial plane in Sec.2, which came out as $r_c \approx 2.4626\sqrt{a}$ (Eq.19). Now, substituting this value in Eq.(61) we obtain the spin precession frequency of the equatorial photon as

$$\vec{\Omega}_p|_{q=1/2, \theta=\pi/2} = \pm \frac{0.2}{\sqrt{a}} \left(1 - \frac{b}{2.4626\sqrt{a}}\right)^{\frac{1}{2}} \hat{\theta}. \quad (62)$$

It indicates that if the throat radius of the wormhole is equal to $2.4626\sqrt{a}$, spin precession vanishes at the throat though it is located in strong gravity regime. This does not arise for $b > 2.4626\sqrt{a}$ because, the precession frequency becomes imaginary and CPO occurs inside the throat but we can always calculate the spin precession of the photon in the opposite case, i.e., $b \leq 2.4626\sqrt{a}$, as CPO occurs outside the throat of a Teo wormhole.

6 Summary and Discussion

In the first part of this article, we have briefly discussed the geodesic structure of the rotating traversable Teo wormhole. Later, we have derived some observables which might be used to detect a rotating wormhole, if it in fact exists. Namely, we have indirectly shown that the ISCO coincides with the throat in Teo wormhole for the prograde rotation, as the effective potential vanishes due to $\ell_0 = 0$ and $\mathcal{E}_0 = 1$ in this case whereas for the retrograde rotation, only one stable circular orbit exists which occurs at the throat. After that, we have derived the fundamental frequencies of a test particle which rotates in an equatorial circular orbit in this rotating wormhole. We have shown that the Kepler frequency (Ω_ϕ) is proportional to r^{-3} in the Teo wormhole but in general it varies with $r^{-\frac{3}{2}}$ in case of

the Kerr black hole and other similar compact objects like pulsars, neutron stars etc. It has also been shown that the Kepler frequency is directly proportional to the angular momentum of the wormhole. Therefore, it vanishes in case of the non-rotating Teo wormhole. Similarly, the nodal plane precession frequency and periastron precession frequency are also proportional to r^{-3} in this case. This can be used to distinguish between a Kerr spacetime and a wormhole spacetime, if the latter in fact exists. Interestingly, the Kepler frequency and the periastron precession frequency behave in a similar fashion due to the vanishing radial epicyclic frequency for the prograde rotation. Thus, we can conclude that the Kepler frequency and periastron precession frequency are actually same in a Teo wormhole.

In the second part, we have shown that the LT precession frequency of a test gyro need not always be directly proportional to the rotation of the wormhole. It behaves differently in the wormhole spacetime. In fact, we have find that the LT precession rate along the pole is inversely proportional to the angular momentum of the wormhole, contrary to our usual expectation that the LT precession rate is not only directly proportional to the rotation of the spacetime but also follows the inverse cube law of distance. Here, we have deduced that the LT precession rate follows an inverse square law of distance along the pole in the strong gravity regime. We believe these to be the crucial factors in observationally distinguishing a wormhole spacetime from that of other compact objects as such an ‘adverse effect’ has not been found in any other spacetimes till now. In our recent study on LT precession in a Kerr spacetime [28], we have demonstrated that the LT precession frequency is never inversely proportional to the rotation of the spacetime outside a Kerr black hole because it should always be proportional to the angular momentum of the spacetime though LT precession acts differently in case of a Kerr naked singularity. Therefore, the distinct behaviors of LT precession may help us to distinguish between wormholes, Kerr black holes and Kerr naked singularities during future astrophysical observation. Further, using the general formulation of spin precession [17], we have derived the spin precession frequency of a test gyro inside and outside the ergoregion of a Teo wormhole. It has been shown that the spin of a gyro precesses not only due to the curvature and the rotation of the spacetime but also due to the non-zero angular velocity of the gyro. This general formulation reduces to the case of a ZAMO for $q = 0.5$ when the spin precession arises purely due to the frame-dragging effect. We have also clearly shown, at least in principle, that there are key and essential theoretical differences that can be used to distinguish a wormhole from a black hole. Finally, we can say that if in future, interstellar traveling through a wormhole or at least in its vicinity becomes possible, our results would give detailed information on the behavior of a test gyroscope which serves as a fundamental navigation device.

Acknowledgements : We thank Oindrila Ganguly for her careful and critical reading of the manuscript.

References

- [1] L. Flamm, *Beitrage zur Einsteinschen Gravitationstheorie*, *Phys. Z. XVII*, (1916) 448
- [2] A. Einstein, N. Rosen, *The Particle Problem in the General Theory of Relativity*, *Phys. Rev.* 48, (1935) 73
- [3] J. A Wheeler, *Geometrodynamics*, Academic, New York, (1962)
- [4] H. G. Ellis, *Ether flow through a drainhole: A particle model in general relativity*, *J. Math. Phys.* **14**, (1973) 104
- [5] K. A. Bronnikov, *Scalar-tensor theory and scalar charge*, *Acta Physica Polonica* **B4**, (1973) 251
- [6] M. S. Morris, K. S. Thorne, *Wormholes in spacetime and their use for interstellar travel: A tool for teaching general relativity*, *Am. J. Phys.* **56**, (1988) 395
- [7] M. S. Morris, K. S. Thorne, U. Yurtsever, *Wormholes, Time Machines, and the Weak Energy Condition*, *Phys. Rev. Lett.* **61** (1988) 1446

- [8] M. Visser, *Traversable wormholes: Some simple examples*, *Phys. Rev. D* **39** (1989) 3182
- [9] G. Clément, *Einstein-Maxwell-Higgs solitons*, *Gen Relat Gravit*, **13** (1981) 747
- [10] G. Clément, *Regular multi-particle solutions of Einstein-Maxwell scalar field theories*, *CQG*, **1** (1984) 275
- [11] G. Clément, *A class of stationary axisymmetric solutions of Einstein-Maxwell scalar field theories*, *CQG*, **1** (1984) 283;
- [12] M. Zhou et al., *Search for astrophysical rotating Ellis wormholes with X-ray reflection spectroscopy*, *arXiv:1603.07448v1* [gr-qc] (2016)
- [13] N. Tsukamoto, C. Bambi, *High energy collision of two particles in wormhole spacetimes*, *Phys. Rev. D* **91**, 084013 (2015)
- [14] N. Tsukamoto, C. Bambi, *Collisional Penrose process in a rotating wormhole spacetime*, *Phys. Rev. D* **91**, 104040 (2015)
- [15] E. Teo, *Rotating traversable wormholes*, *Phys. Rev. D* **58**, 024014 (1998).
- [16] C. Chakraborty, P. Majumdar, *Strong gravity Lense-Thirring precession in Kerr and Kerr-Taub-NUT spacetimes*, *CQG* **31**, (2014) 075006
- [17] C. Chakraborty, M. Patil, P. Kocherlakota, S. Bhattacharyya, P. S. Joshi, A. Królak, *Distinguishing Kerr naked singularities and black holes using the spin precession of a test gyro in strong gravitational fields*, *arXiv:1611.08808v1* [gr-qc] (2016)
- [18] S. Chandrasekar, *The Mathematical Theory of Black Holes*, Clarendon Press, Oxford (1983)
- [19] P. Pradhan, *Circular geodesics in the Kerr-Newman-Taub-NUT spacetime*, *Class. Quantum Grav.* **32**, 165001 (2015)
- [20] D. D. Doneva et al., *Orbital and epicyclic frequencies around rapidly rotating compact stars in scalar-tensor theories of gravity*, *Phys. Rev. D* **90**, (2014) 044004
- [21] J. Lense and H. Thirring, *Ueber den Einfluss der Eigenrotation der Zentralkörper auf die Bewegung der Planeten und Monde nach der Einsteinschen Gravitationstheorie* *Phys. Z.* **19**, (1918) 156.
- [22] L. I. Schiff, *Possible New Experimental Test of General Relativity Theory*, *PRL* **4**, (1960) 215; L. I. Schiff, *On Experimental Tests of the General Theory of Relativity*, *American Journal of Physics*, **28**, (1960) 340
- [23] C. W. F. Everitt et al., *Gravity Probe B: Final Results of a Space Experiment to Test General Relativity*, *PRL*, **106**, (2011) 221101 ; C.W.F. Everitt et al., *The Gravity Probe B test of general relativity*, *Class. Quantum Grav.* **32** (2015) 224001
- [24] C. Chakraborty, P. Pradhan, *Lense-Thirring precession in Plebański-Demiański Spacetimes*, *Eur. Phys. J. C* **73**, (2013) 2536
- [25] C. Chakraborty, K. P. Modak, D. Bandyopadhyay, *Dragging of Inertial Frames inside the Rotating Neutron Stars*, *ApJ* **790**, (2014) 2
- [26] C. Chakraborty, *Anomalous Lense-Thirring precession in Kerr-Taub-NUT spacetimes*, *EPJC* **75**, (2015) 572
- [27] D. Chatterjee, C. Chakraborty, D. Bandyopadhyay, *Gravitomagnetic effect in magnetized neutron stars*, *JCAP* **01**(2017)062, *arXiv:1607.05600* [astro-ph.HE]

- [28] C. Chakraborty, P. Kocherlakota, P. S. Joshi, *Spin precession in a black hole and naked singularity spacetimes*, *PRD* **95**, (2017) 044006, arXiv:1605.00600 [gr-qc]
- [29] S. A. Hojman, F. A. Asenjo, *Can gravitation accelerate neutrinos?*, *Class. Quantum Grav.* **30**, (2013) 025008
- [30] C. Armaza, M. Banados, B. Koch, *Collisions of spinning massive particles in a Schwarzschild background*, *Class. Quantum Grav.* **33**, (2016) 105014
- [31] J. M. Bardeen, *A Variational Principle for Rotating Stars in General Relativity*, *Astrophys. J* **162**, (1970) 71
- [32] C. W. Misner, K. S. Thorne, J. A. Wheeler, *Gravitation*, *W. H Freeman & Company* (1973)
- [33] J. M. Bardeen, W. H. Press, and S. A Teukolsky, *Rotating black holes: Locally nonrotating frames, energy extraction, and scalar synchrotron radiation*, *Astrophys J.* **178**, (1972) 347
- [34] B. F. Schutz, *A First Course in General Relativity*, 2nd Edition, *Cambridge University Press*, (2009)
- [35] S. M. Morsink, L. Stella, *Relativistic Precession around Rotating Neutron Stars: Effects Due to Frame Dragging and Stellar Oblateness*, *ApJ* **513**, (1999) 827